ACS OMEGA

Open Access

http://pubs.acs.org/journal/acsodf

Article

Exploring the Molecular Mechanism of Schisandrin C for the Treatment of Atherosclerosis via the PI3K/AKT/mTOR Autophagy Pathway

Hong Duan,[⊥] Han Li,[⊥] Tianyi Liu, Yuan Chen, Mengmeng Luo, Ying Shi, Jing Zhou, Marwan M. A. Rashed, Kefeng Zhai,* Lili Li,* and Zhaojun Wei*

Cite This: *ACS Omega* 2024, 9, 32920−32930

Read Online

ACCESS | Metrics & More | Article Recommendations

ABSTRACT: Atherosclerosis (AS) is a common cardiovascular disease that poses a major threat to health. *Schisandra chinensis* is a medicinal and edible plant that is commonly used to treat cardiovascular diseases. In this paper, HPLC was used to detect and analyze 5 different components in *Schisandra chinensis*. Network pharmacological predictions highlight the PI3K/AKT/mTOR pathway as an important pharmacological pathway. The effective ingredient Schisandrin C was screened by the molecular docking technique. ox-LDL-induced HUVECs were used to construct the atherosclerosis model for further experimental verification. The results showed that Schisandrin C interfered with the PI3K/AKT/mTOR autophagy pathway. This study lays a foundation for the further application of Schisandrin C in the prevention and treatment of atherosclerosis in the future.

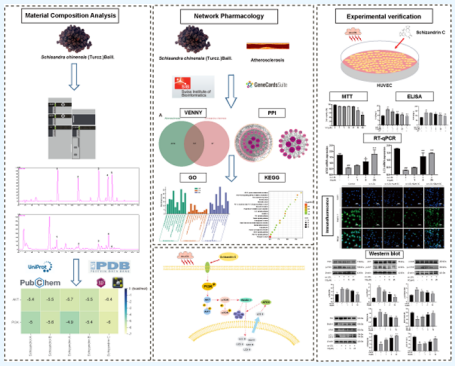

INTRODUCTION

Cardiovascular disease (CVD) is one of the most serious diseases that endanger human health in the world and has become the first cause of death in human beings.[1] Atherosclerosis (AS) is one of the main causes of cardiovascular disease, and its pathogenesis is a complex process involving multiple cellular and molecular interactions.[2] Lipid metabolism disorder is one of the main pathogeneses of atherosclerosis.[3] In the case of lipid metabolism disorders, lipid substances such as cholesterol and triglycerides in the blood can be deposited in the walls of blood vessels, forming lipid plaques.[4] The formation of lipid plaques can cause the gradual thickening of the blood vessel wall and the narrowing of the vessel lumen, affecting the flow of blood and oxygen supply.[5] In response to inflammation, low-density lipoprotein (LDL) is oxidized within the blood vessel wall to form oxidized low-density lipoprotein (ox-LDL).[6]

Schisandra chinensis (Turcz.) is the dried fruit of *Schisandra chinensis* (Turcz.) Baill. Sour, sweet, warm, and non-toxic, it was originally published in Shennong Herbal Classic,[7] and is a kind of Chinese herbal medicine, also known as "medicine and food homologous" plant. The homology of medicine and food refers to that some plants can be used as both drugs and food and have the effect of both medicine and food. *Schisandra chinensis* is widely used in traditional Chinese medicine. It has the functions of astringent, invigorating qi and promoting fluid, tonifying the kidney, calming the heart, etc.[8] It is an important medicinal taste of Chinese traditional medicine compound for "invigorating qi and nourishing Yin". *Schisandra chinensis* regulates blood lipids, lowering total cholesterol, triglycerides, and LDL cholesterol while increasing HDL cholesterol levels.[9] Therefore, it has a protective effect on cardiovascular diseases, and *Schisandra chinensis* is commonly used in Chinese medicine to treat cardiovascular diseases.[10] Clinical observation shows that adding *Schisandra chinensis* to conventional treatment can significantly improve heart function and relieve anxiety in patients recovering from myocardial infarction, which has dual effects of medical care.[11] Hyperlipidemia is an important cause of arteriosclerotic diseases. *Schisandra chinensis* lignans can reduce the levels of TC, TG, and LDL in rat serum and increase the content of HDL, which has the effect of treating hyperlipidemia.[12] Schisandrin C (SC) is a biphenyl cyclooctadiene lignan isolated from *Schisandra chinensis*.[13] Recently, we found that SC has a good cardio-cerebrovascular protective effect.

Autophagy involves the phagocytosis of cytoplasmic proteins or organelles, fusion with lysosomes to create autophagic lysosomes, and subsequent degradation and reuse.[14] Autophagy

Received: April 19, 2024
Revised: June 16, 2024
Accepted: July 2, 2024
Published: July 16, 2024

is divided into three main categories: macroautophagy, microautophagy, and chaperone-mediated autophagy (CMA).[15] Autophagy is an intracellular protective mechanism that maintains cellular homeostasis by breaking down and removing harmful substances and damaged organelles within the cell.[16] Studies have shown that autophagy plays an important role in the occurrence and development of atherosclerosis.[17] Autophagy can remove abnormal lipid substances in the cell, such as oxidized lipids and phospholipids, so as to maintain the homeostasis of intracellular lipid metabolism.[18] Autophagy can affect the synthesis and degradation of intracellular lipids by regulating the signaling pathways related to lipid synthesis and degradation so as to maintain the balance of lipid metabolism.[19] Autophagy can affect the metabolism of cholesterol by degrading cholesterol esterase and other related enzymes, thus regulating the level of intracellular cholesterol.[20] Autophagy can remove oxidized lipid substances and reduce the generation of oxidative stress, thus inhibiting the occurrence of inflammatory response and playing a protective role in lipid metabolism.[21] In general, autophagy plays an important role in the regulation of intracellular lipid metabolism by clearing abnormal lipid substances, regulating lipid synthesis and degradation, affecting cholesterol metabolism, and inhibiting oxidative stress and inflammation.

MATERIALS AND METHODS

Materials and Chemicals. North *Schisandra chinensis* sample (lot number: N20230224) was purchased from Baicao Pharmaceutical Co., Ltd. Glacial acetic acid, chromatographic grade methanol, chromatographic grade acetonitrile, and Atorvastatin (AT) (batch numbers are A116167, M433281, A119010, and A420607, respectively) were purchased from Shanghai Aladdin Biochemical Technology Co., Ltd. Schisandrol A standard, Schisandrol B standard, Schizandrin A standard, Schizandrin B standard, and Schizandrin C standard were all (batch numbers were Yz170617, Yz051522, Yz031020, Yz101722, and Yz1207221, respectively) purchased from Nanjing Yuanzhi Biotechnology Co., Ltd..

HUVECs were purchased from Wuhan Punosai Life Technology Co., Ltd. BCA protein concentration quantitative kit (lot number E112-01) was purchased from Shanghai Biyuntian Biotechnology Co., Ltd. Human interleukin-1β (IL-1β batch no. YFXEH00259), human tumor necrosis factor-α (TNF-α batch No. YFXEH00034), ELISA kit, total RNA rapid extraction reagent (including RNApure) (batch no. YFXM0011P), cDNA the first-chain Rapid synthesis kit (Degenomic) (lot No. YFXM0012), and 2 × SYBR Green Fast qPCR Master Mix (lot No. YFXM0001) were purchased from YIFEIXUE Biotech Co., Ltd. RIPA lysate (lot No. E311-02) was purchased from Nanjing Vazyme Biotech Co., Ltd. Primary antibodies protein kinase B (AKT), phospho-protein kinase B (p-Akt), phosphoinositide 3-kinase (PI3K), mammalian target of rapamycin (mTOR), phospho-mammalian target of rapamycin (p-mTOR), ATG5, Beclin1, microtubule-associated protein 1 light chain 3 (LC3), β-actin (β-actin), rabbit and mouse (lot numbers: 60203−2-Ig, 66444−1-Ig, 20584−1-AP, 66888−1-Ig, 67778−1-Ig, 10181−2-AP, 11306−1-AP, 14600−1-AP, 66009−1-Ig, SA0001−2, and SA0001−1) were purchased from Proteintech Company; Phospho-phosphoinositide 3-kinase (p-PI3K) (lot number BS4605) was purchased from Bioworld; P62 (lot number ab109012) was purchased from Abcam Company; the sequence of primers synthesized from General Biology Co., Ltd. is shown in Table 1; and oxidized low-density lipoprotein (Lot No. YB-002) was purchased from Yiyuan Biological Co., Ltd.

Table 1. Primers Sequence

primer name	sequence (5′ to 3′)
ATG5-F	CTGGGCTGGTCTTACTTTGC
ATG5-R	GGCCAAAGGTTTCAGCTTCA
LC3-F	AACATGAGCGAGTTGGTCAAG
LC3-R	GCTCGTAGATGTCCGCGAT
18S−F	AAACGGCTACCACATCCAAG
18S-R	CCTCCAATGGATCCTCGTTA

Analysis of Material Components in Extracts of *Schisandra chinensis*. *Preparation of Schisandra chinensis.* 5.000 g of the prepared *Schisandra chinensis* powder was added to 100 mL of anhydrous ethanol in a round-bottom flask according to the solid−liquid ratio of 1:20 (g/mL), extracted by hot reflux extraction method for 2.5 h, and then filtered to collect the filtrate. The obtained solution is the extract of *Schisandra chinensis*.

HPLC Analysis of Schisandra chinensis Extract. The chromatography was performed on A shim-pack C18 ODS column (200 mm × 4.6 mm, 5 μm) with acetonitrile (A) −0.5% acetic acid solution (B) as the mobile phase in a high-performance liquid chromatography (Shimadsu LC20AD). The column temperature was set at 30 °C, and the total flow rate was adjusted to 0.8 mL/min. The wavelength is set to 254 nm, and the sample size was 20 μL. The elution time program is shown in Table 2.

Table 2. Gradient Elution Time Program

time (min)	acetonitrile (%)	0.5% acetic acid solution (%)
0	45	55
5	50	50
15	60	40
25	70	30
30	80	20
40	85	15
45	Stop	

Network Pharmacological Analysis and Molecular Docking. *Potential Target Schisandra chinensis and Atherosclerotic.* Based on the component information of HPLC analysis and molecular docking screening, the obtained component was imported into the PubChem database (https://pubchem.ncbi.nlm.nih.gov/) to obtain the component information, and the obtained result was imported into the SwissTargetPrediction database (http://new.Swisstargetprediction.ch/) to predict the target of the component. Using the OMIM (http://www.omim.org/) and Gene Cards database (https://www.genecards.org/) with the keyword "Atherosclerosis", the potential target of relevant disease was searched to obtain the disease target associated with skin inflammation. The components were matched with the relevant targets of atherosclerosis, and the Venn Diagram was drawn using the online drawing website Draw Venn Diagram.[22]

Protein−Protein Interaction (PPI) Network. To clarify the interaction between disease and component targets, the common targets were imported into the String database (https://cn.string-db.org/), and the PPI network model with biological species set as "Human" was constructed. When

https://doi.org/10.1021/acsomega.4c03738
ACS Omega 2024, 9, 32920−32930

confidence degree >0.7, the node was hidden where the network is disconnected, and the remaining parameters were set to their default values. The data map of the protein interaction is obtained and saved in TSV format, which is then imported into Cytoscape 3.8.2 software for protein interaction (PPI) visualization.[23]

Gene Enrichment Analysis. Common target will import DAVID database (https://david.ncifcrf.gov/), with $P < 0.05$, FDR < 0.05, for the filter condition, selection of *Homo sapiens* (*Homo sapiens*) species "Gene-Ontology" get the GO entry. Items including Biological Process (BP), Cellular Component (CC), and Molecular Function (MF) were selected as the top 10 in GO analysis. The KEGG-PATHWAY enrichment analysis was conducted to obtain the Kyoto Encyclopedia of Genes and Genomes (KEGG) signal pathway, and graphs were drawn for the top 20 items in KEGG analysis.[24] A microscopic letter database (https://www.bioinformatics.com.cn/) will be visualized analysis results.[25]

Molecular Docking. The CAS numbers of five active ingredients of *Schisandra schisandra* were input into the PubChem database, and the 2D structure in SDF format was downloaded. After minimum energy processing, the files were imported into Chem 3D and saved in mol2 format. Search for the core target name in the UniProt database (https://www.uniprot.org/) and select "human" to copy its entry name. The entry name of the core target was searched in the PDB database (https://www.rcsb.org/) and downloaded the target file. AutoDock software was used first to introduce two core proteins for water removal hydrogenation treatment, AutoDockTools was used to hydrogenate five active ingredients, AutoDockVina was used for molecular docking of active ingredients and core targets, and PyMol software was used for visual analysis.[26]

Cell Assays. *Cell Culture.* HUVECs were cultured in DMEM containing 10% fetal bovine serum and 1% penicillin-streptomycin antibiotic in an incubator at 37 °C and 5% CO_2. When the cells in the culture dish grew to 90%, passage was performed. The cells were digested with pancreatic enzyme and blown down, then collected into a centrifuge tube, centrifuged at 1100 rpm/min for 4 min. The supernatant was discarded, and the cells were resuspended by adding fresh medium for passage.

Effects of Schizandrin C on HUVEC Cell Viability. HUVECs were cultured with DMEM medium containing 10% fetal bovine serum. The cell concentration was adjusted, and the cells were inoculated into 96-well plates at the rate of 2×10^4 cells per well. Cultured at 37 °C and 5% CO_2 for 24 h, the supernatant was discarded and cultured in the medium containing different concentrations of Schizandrin C with the final concentration of 0, 1, 5, 10, 25, 50, 100 μM, and 6 holes were repeated. After culture for 24 h, 5 mg/mL MTT 20 μL was added to each well. After continuous culture for 4 h, the supernatant was carefully discarded, DMSO was added to 150 μL per well, and the absorbance was measured at 490 nm on the enzyme marker after shaking for 8 min.

Expression of IL-1β and TNF-α in Cell Supernatant Detection Using ELISA. HUVECs were inoculated in a 6-well cell culture plate and cultured at 37 °C for 24 h. Except the blank control group, 50 μg/mL ox-LDL was added to each well in the other groups, while the drug group was given different concentrations of Schizandrin C, and the positive control group was added with 1 μM AT for 24 h. The cell supernatant was collected in a centrifuge tube at 4 °C, 3000 rpm/min and centrifuged for 15 min. The supernatant was obtained, and the expression levels of IL-1β and TNF-α in the cell supernatant were detected by ELISA kit.[27]

Beclin1 Expression Using the Immunofluorescence Method. HUVECs were inoculated in a confocal dish with 1.5×10^5 cells/dish, and HUVEC was cultured with DMEM medium containing 10% fetal bovine serum. After the cells were affixed to the wall, 50 μg/mL ox-LDL and different concentrations of Schisandrin C were added to the culture for 24 h. Then, the supernatant was discarded, washed twice with PBS, fixed with fixing solution for 30 min, washed three times with PBS, and treated with detergent for 5 min. After washing with PBS, 5% BSA was added and closed for 1 h, Beclin1 antibodies were added, incubated at 4 °C for one night, washed with PBS and treated with fluorescent secondary antibody for 1 h, cleaned with DAPI for 5 min, washed with PBS, added with an antifluorescence quencher, and then photographed under a confocal laser microscope.

Western Blot Expression of Autophagy Signaling Pathway-Related Proteins. HUVECs were inoculated with 2×10^6 cells/dish in a 60 mm^2 cell culture dish, and HUVECs were cultured with DMEM medium containing 10% fetal bovine serum. After the cells were affixed to the wall, 50 μg/mL ox-LDL and different concentrations of Schizandrin C were added for 24 h, the super serum was discarded, and the RIPA lysate containing phenylmethylsulfonyl fluorid (PMSF) was added to collect cells and extract proteins. The protein concentration was determined by the BCA protein quantitative method, and the protein was isolated by SDS-PAGE electrophoresis and transferred to the PVDF membrane. Diluted β-actin, AKT, p-AKT, PI3K, p-PI3K, mTOR, p-mTOR, ATG5, Beclin1, LC3, P62, and primary antibody were added and incubated overnight. After incubation, the second antibody labeled with HRP was added and incubated at room temperature for 2 h. The chemiluminescence imaging system was used to image and take photos for ECL luminescence detection, and the gray value was calculated by ImageJ software.

Detection mRNA Expression of Related Genes Using RT-qPCR. Total RNA Extraction. Trizol was added to the cells and left at room temperature for 5 min to fully lyse the cells. Then, chloroform was added to the cells and mixed well. The upper colorless water phase was centrifuged into a new centrifuge tube, and isopropyl alcohol was added in equal volume and reverse-mixed several times. Again, the supernatant was centrifuged and discarded. Then, 75% ethanol (prepared with DEPC water) was added, cleaned, precipitated, and dissolved the RNA after slightly drying. Finally, 20 μL of DEPC water was added.

cDNA Synthesis. The experiment was performed using the cDNA first-strand rapid synthesis kit (Degenomic). A total of 1 μg RNA, one μL gDNA Eraser, and 8 μL DNase/RNase-Free Water were mixed, incubated at 42 °C for 5 min, and placed on ice to obtain genomic DNA removal reaction solution. 10 μL of genomic DNA removal reaction solution and 2x first-strand cDNA synthesis super mix were taken, respectively, gently mixed, briefly centrifuged, and incubated at 50 °C for 15 min. The enzyme was inactivated at 75 °C for 5 min. The 1 μL template solution was directly used for the subsequent PCR experiment.

Fluorescence Quantitative PCR Was Used to Detect Relative Expression Levels. Using 18s as the internal reference, General Biotechnology Co., Ltd., synthesized human mRNA primers, and their sequences are shown in Table 1. The following reagents were added according to the following reaction system (20 μL reaction system): cDNA template 1 μL,

https://doi.org/10.1021/acsomega.4c03738
ACS Omega 2024, 9, 32920−32930

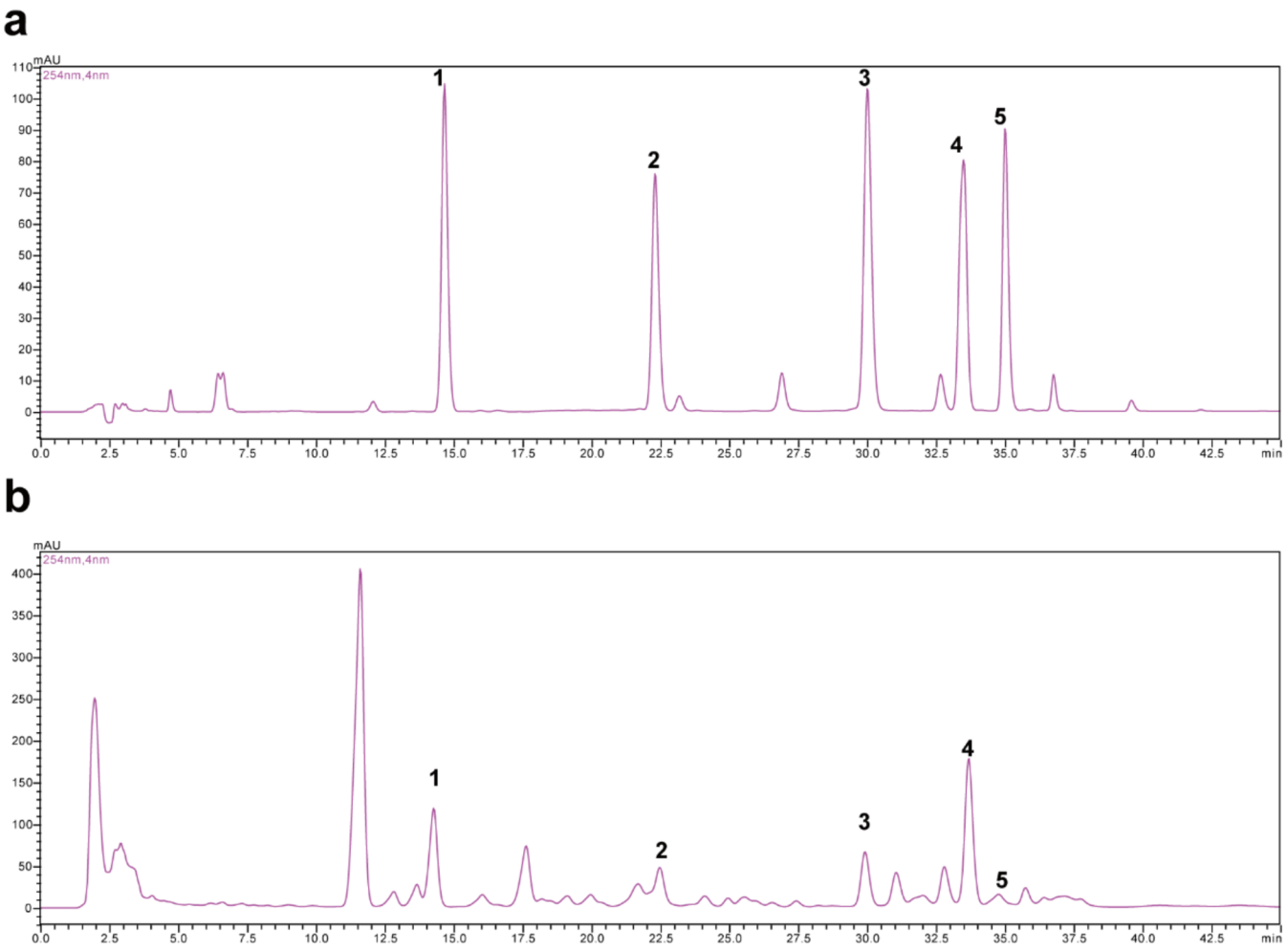

Figure 1. (a) Chromatogram of mixed standard products. (b) Chromatogram of *Schisandra chinensis* extract (1, Schisandrol B; 2, Schisandrol A; 3, Schizandrin A; 4, Schizandrin B; and 5, Schizandrin C).

Table 3. Standard Curves of Each Standard Product

ingredient	regression equation	determination coefficient (r^2)	linear range μg/mL
Schisandrol A	$y = 33349x + 96352$	1	27.600−230.000
Schisandrol B	$y = 46774x - 180.1$	0.9999	3.520−176.000
Schizandrin A	$y = 49494x + 136231$	0.9999	3.200−384.000
Schizandrin B	$y = 54401x + 5462$	0.9999	2.940−147.000
Schizandrin C	$y = 40552x + 3544.1$	0.9999	3.400−34.000

forward primer 0.5 μL, reverse primer 0.5 μL, 2 × SYBR Green Fast qPCR Master Mix-LR 10, DEPC water 8 μL. Experiment was performed on Applied Biosystems ViiA 7 (real-time PCR amplification apparatus).

Statistical Analysis. The data were imported into GraphPad Prism 8.0.2 for calculation and processing, and the significance of the detected data was analyzed by Student t-test or ANOVA. The results were presented in the form of mean ± standard error ($\bar{X} \pm$ SEM). A P value of <0.05 ($p < 0.05$) was considered for the significant difference and denoted by (*), whereas the significance level with a p value of <0.01 ($p < 0.01$) was denoted by (**).

RESULTS

Composition Identification of *Schisandra chinensis*. The components of *Schisandra chinensis* and the standard solution were analyzed and detected according to the detection conditions given in Table 2. The separation effect of the target component is shown in Figure 1a, where Figure 1a is the HPLC chromatogram of the mixed standard, and Figure 1b is the composition sample of *Schisandra chinensis*. The separation degree of each peak is good, indicating that the chromatographic condition has a good separation effect on the sample and the standard. The results showed that there were rich chemical components in *Schisandra chinensis*, among which five active components were identified by comparison of standard substances, which were Schisandrol A, Schisandrol B, Schisandrin A, Schisandrin B, and Schisandrin C. The chromatographic diagram is shown in Figure 1b.

Linearity, precision, reproducibility, stability, and recovery rate were evaluated. The results showed that Schisandrol A, Schisandrol B, Schizandrin A, Schizandrin B, and Schizandrin C had a good linear relationship in the linear range, and the correlation coefficient r^2 of the linear relationship was above

https://doi.org/10.1021/acsomega.4c03738
ACS Omega 2024, 9, 32920−32930

0.99, as shown in Table 3. The precision, reproducibility, stability, and relative standard deviation (RSD) of standard recovery were all less than 2%. The results are within the acceptable range. The above results show that the method is feasible for the analysis of *Schisandra chinensis* extract. Combined with the results of linear relationship, the contents of each substance in the extract of *Schisandra chinensis* were calculated to be 23.236, 54.485, 27.504, 69.864, and 13.761 μg/mL, respectively, and the experimental results are shown in Table 4.

Table 4. Content of Components in Extracts of *Schisandra chinensis* (n = 3)

ingredient	peak area $\bar{y}$	mean content $\bar{x}$ (μg/mL)
Schisandrol A	1 371 478	38.236
Schisandrol B	2 548 299	54.485
Schizandrin A	1 497 506	27.504
Schizandrin B	3 806 154	69.864
Schizandrin C	561 592	13.761

Prediction of Mechanism of Action of *Schisandra chinensis* Components on Atherosclerosis by Network Pharmacology. According to the five active components of *Schisandra chinensis* obtained by liquid chromatography analysis, the 2D structure was searched through PubChem database, and the target of the five components was predicted through SwissTargetPrediction database. The result showed that there were 284 target points of the five components of *Schisandra chinensis* after removing duplications. Using "atherosclerosis" as the keyword, a total of 5113 potential targets for related diseases were searched. The component targets of *Schisandra chinensis* were matched with atheromatosis-related targets, and Venn plots were drawn using an online mapping website (Figure 2a). The results showed that there were 197 common targets between five components of *Schisandra chinensis* and atherosclerosis. The interaction network diagram between *Schisandra chinensis* components and atherosclerotic proteins was established by Cytoscape software (Figure 2b). The results showed that potential targets of *Schisandra chinensis* associated with atherosclerosis include SRC, STAT3, HSP90AA1, AKT1, EGFR, PIK3CA, and PIK3R1. KEGG pathway enrichment analysis was performed on 197 targets obtained from DAVID database. A total of 177 KEGG signal pathways were obtained after enrichment. By setting $P < 0.05$ and FDR < 0.05, the top 20 entries are shown in Figure 2c. The findings suggest that this is related to various pathways such as pathways in cancer, AGE-RAGE signaling pathway in diabetic complications, Hepatitis B, proteoglycans in cancer, prostate cancer, EGFR tyrosine kinase inhibitor resistance, Kaposi sarcoma-associated herpesvirus infection, PI3K-Akt signaling pathway, FoxO signaling pathway, MAPK signaling pathway, etc. GO enrichment analysis was performed on 197 targets obtained by using DAVID database. We found 773 Biological Process (BP) items, including protein phosphorylation, protein autophosphorylation, peptidyl-serine phosphorylation, peptidyl-threonine phosphorylation, inflammatory response, etc.; 108 Cellular Component (CC) entries, including plasma membrane, receptor complex, integral component of plasma membrane, membrane raft, cell surface, etc.; and 158 molecular function (MF) entries, including protein serine/threonine/tyrosine kinase activity, protein kinase activity, ATP binding, protein tyrosine kinase activity, protein serine/threonine kinase activity, etc. These articles explore various aspects of molecular function. The result is shown in Figure 2d. After the results of KEGG pathway analysis, the target in the pathway was mapped to the compound, and the "composition-target-pathway" network diagram was constructed. The results showed that schisandra can act on multiple compounds and targets in multiple ways to achieve the therapeutic effect of atherosclerosis, as shown in Figure 2e.

Molecular Docking Predicted the Binding Force of Different Components of *Schisandra chinensis* and Core Target. The receptor proteins of key AKT and PI3K targets were obtained in the PDB database, and the secondary structures of five active components of *Schisandra chinensis* were obtained in the PubChem database. The key target protein and five active components of *Schisandra chinensis* were separately treated for molecular docking analysis, and the binding free energy of the docking was obtained, as shown in Figure 3k. The docking results were imported into PyMol for visual analysis, as shown in Figure 3a−j. The lower the binding energy is, the more stable the binding of ligand and receptor is, and the binding energy less than 0 indicates spontaneous binding. The binding energy is less than −5 kcal·mol^{-1} as the scoring criterion.[28] The results showed that the binding force between the five active components of *Schisandra chinensis* and the key targets was less than −5 kcal·mol^{-1}, except for the binding energy of −4.9 kcal·mol^{-1} between Schizandrin A and PI3K. Therefore, the five active components of *Schisandra chinensis* can bind to the key targets of AKT and PI3K. Among them, Schizandrin C has the best binding effect on AKT and PI3K key targets.

Effects of Schizandrin C on Cell Activity. As shown in Figure 4a, HUVECs were treated with different concentrations of Schisandrin C, the drug concentration was screened, and the effect of different concentrations of Schizandrin C on cell viability was detected by the MTT method. The results showed that different concentrations of Schizandrin C had effects on HUVECs. When the concentration of Schizandrin C was higher than 25 μM, it had significant toxic effects on HUVECs. Therefore, the drug concentration below 25 μM was selected in the follow-up experiment.

Effect of Schizandrin C on ox-LDL-Induced Cytokine Release in HUVECs. In order to further verify the effect of Schisandrin C on the release of inflammatory factors in ox-LDL-induced HUVECs, the cell supernatant of different groups was taken, and the inflammatory factors of TNF-α and IL-1β cells were detected by ELISA kit. The figure illustrates the results. In contrast to the normal control, ox-LDL significantly increased IL-1β and TNF-α. However, Schisandrin C administration notably reduced TNF-α and IL-1β compared to the ox-LDL group. Compared with the ox-LDL group, the expression levels of TNF-α and IL-1β were significantly decreased in the medium and high-dose administration groups of Schisandrin C (Figure 4**b**,**c**). It is suggested that Schisandrin C can significantly reduce the expression level of inflammatory factors in HUVECs and alleviate the inflammatory response.

Effect of Schisandrin C on the ox-LDL-Induced Autophagy of HUVECs Using Immunofluorescence. In this study, the related expression of Beclin1, a key protein of the autophagy pathway, was further detected in HUVECs by the immunofluorescence method. As shown in Figure 4d, the histone expression level of the ox-LDL-induced model decreased, Schisandrin C significantly increased the expression level of autophagy protein Beclin1. The results showed that

https://doi.org/10.1021/acsomega.4c03738
ACS Omega 2024, 9, 32920−32930

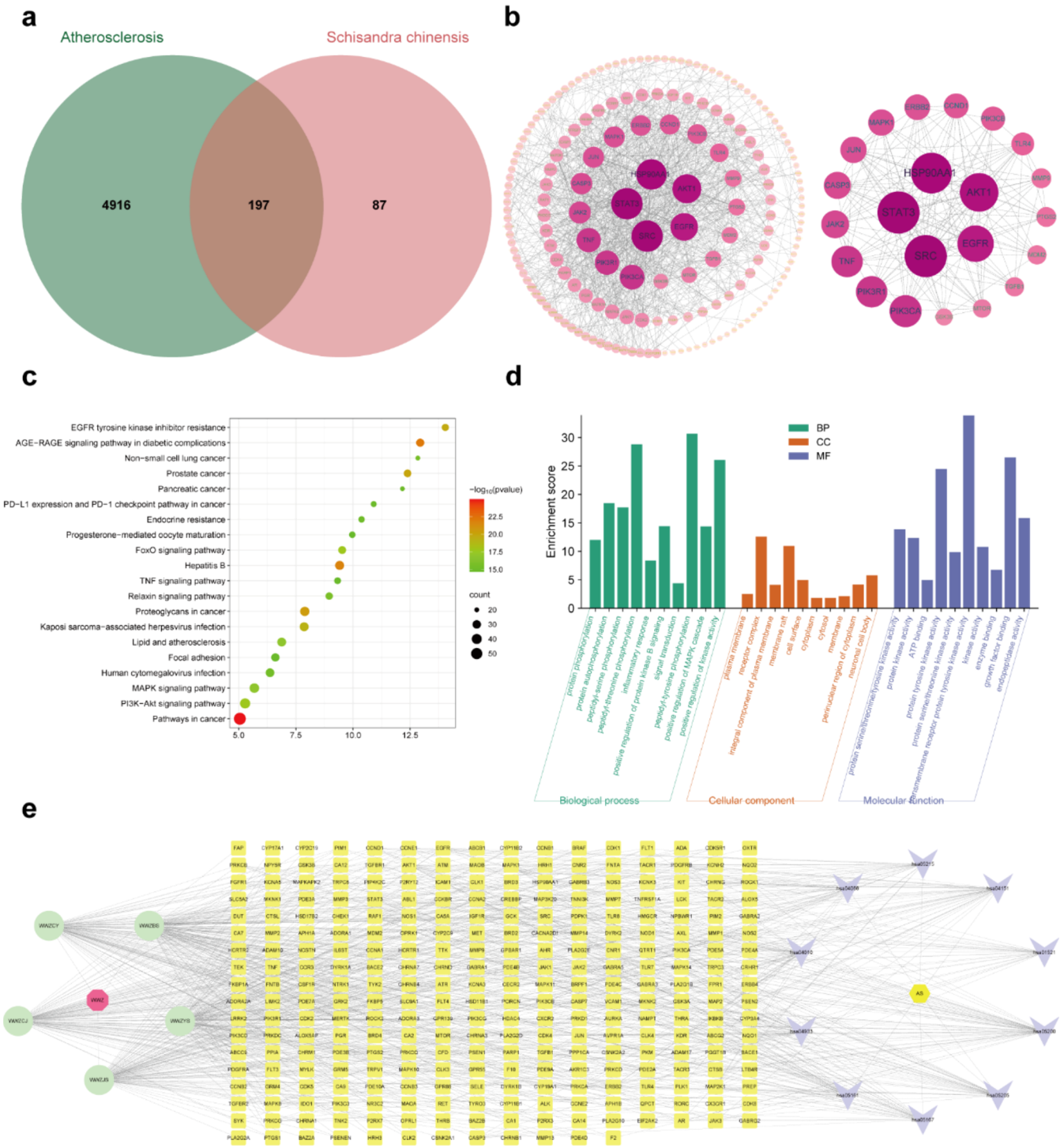

Figure 2. Relationship between five components of *Schisandra chinensis* and atherosclerosis was analyzed by network pharmacology. (a) Venn diagram of *Schisandra chinensis* and atherosclerotic disease targets; (b) interaction network between *Schisandra chinensis* and atherosclerotic target proteins; (c) KEGG enrichment analysis of *Schisandra chinensis* for the treatment of atherosclerotic targets; (d) GO analysis results of *Schisandra chinensis* in treating atherosclerosis targets; and (e) *Schisandra chinensis* target pathway map.

Schisandrin C could promote autophagy by regulating the expression of autophagy protein in cells.

Confirmation of the PI3K/Akt/mTOR Autophagy Signaling Pathway. Western Blot was used to detect whether Schizandrin C can promote autophagy through the autophagy signaling pathway PI3K/Akt/mTOR. Compared with the control group, PI3K, Akt, and mTOR were significantly phosphorylated in the ox-LDL-induced model group and significantly inhibited the phosphorylation of PI3K/Akt/mTOR protein in a dose-dependent manner after the intervention of Schizandrin C. As shown in Figure 5a−c. These results suggest that autophagy is promoted through the PI3K/Akt/mTOR pathway and is involved in downstream molecular mechanisms.

Expression Levels of Beclin1, LC3 II/LC3 I, ATG5, and P62 Proteins in the Cells Were Detected by Western Blot.

https://doi.org/10.1021/acsomega.4c03738
ACS Omega 2024, 9, 32920−32930

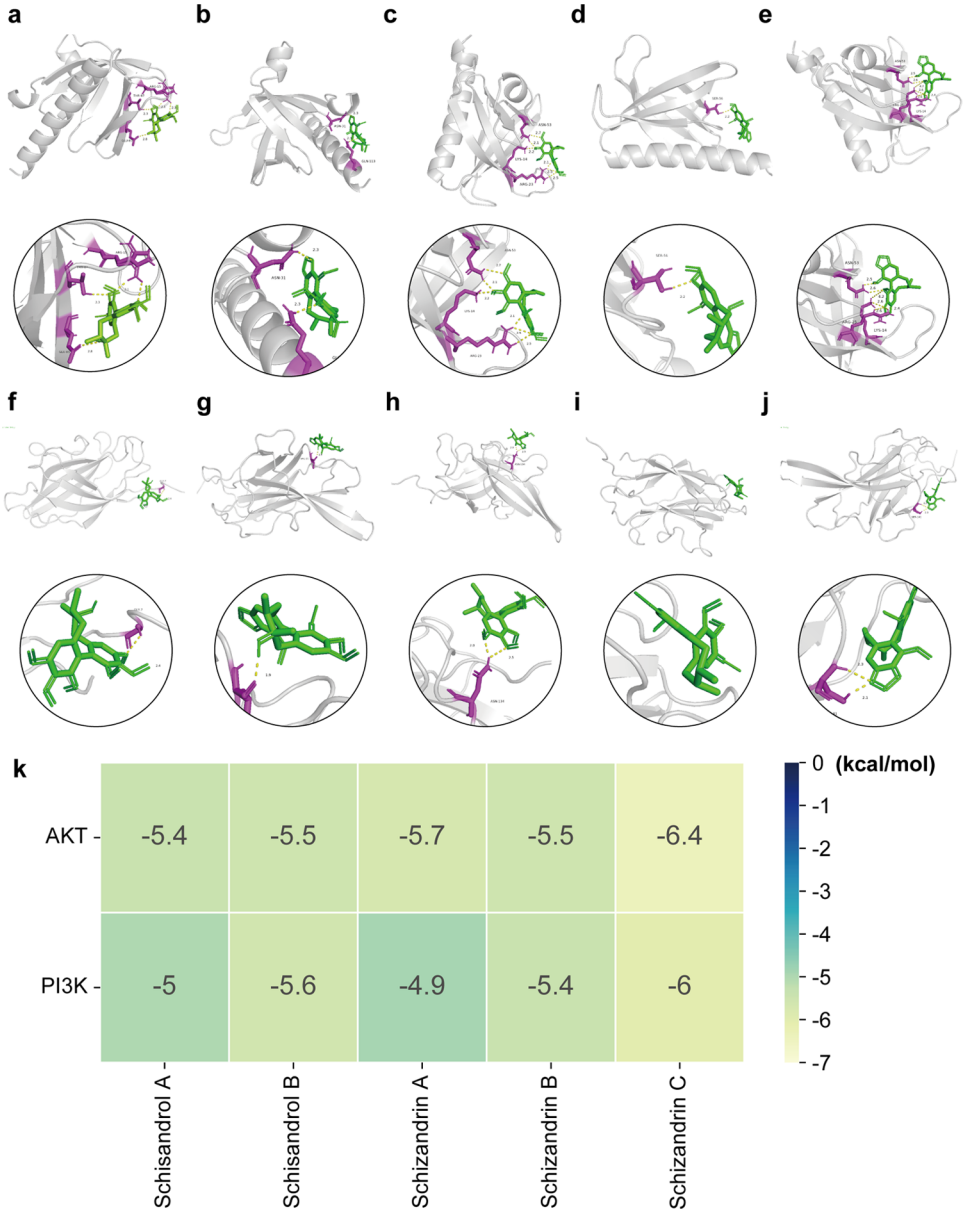

Figure 3. Docking of five active components of *Schisandra chinensis* with core target molecules. (a) AKT-Schisandrol A; (b) AKT-Schisandrol B; (c) AKT-Schizandrin A; (d) AKT-Schizandrin B; (e) AKT-Schizandrin C; (f) PI3K-Schisandrol A. (g) PI3K-Schisandrol B; (h) PI3K-Schizandrin A; (i) PI3K-Schizandrin B; (j) PI3K-Schizandrin C; (k) docking result.

Beclin1 and ATG5 play an important role in the initiation and formation of autophagy. LC3 II is commonly used as a marker of autophagy formation and an important multisignal transduction regulatory protein located on the autophagy cell membrane. The LC3 II/LC3 I ratio can estimate the level of autophagy. At the same time, P62 is a substrate protein involved in the degradation process of autophagy contents and is constantly broken down during autophagy. The analysis of proteins involved in different stages of autophagy helps to determine the fluency of the autophagy pathway. Compared with the blank control group, the expression of the P62 protein was increased in the model group, suggesting that ox-LDL could induce the block of autophagy. The P62 protein was significantly downregulated in the medium and high-dose groups of Schisandrin C, as shown in Figure 6b. Compared with the model group, the Beclin1 protein expression level in the drug groups of Schizandrin C was significantly increased, as shown in Figure 6c. The expression level of ATG5 protein was significantly increased, as shown in Figure 6d. The LC3 II/LC3 I protein was significantly elevated, as shown in Figure 6e. It is suggested that Schisandrin C can increase the level of autophagy and significantly improve the blocking of the autophagy pathway.

Detection of the Expression of LC3 and ATG5 mRNA in Cells Using RT-qPCR. In order to further verify the effect of Schisandrin C on autophagy in ox-LDL-induced HUVECs, mRNA expression levels of autophagy-related genes LC3 and ATG5 in cells were investigated by RT-qPCR. The results are shown in the figure. The mRNA expression levels of LC3 and ATG5 were significantly increased in the medium- and high-dose groups of Schisandrin C, as shown in Figure 7a,b. The results are consistent with Western Blot experiment.

https://doi.org/10.1021/acsomega.4c03738
ACS Omega 2024, 9, 32920−32930

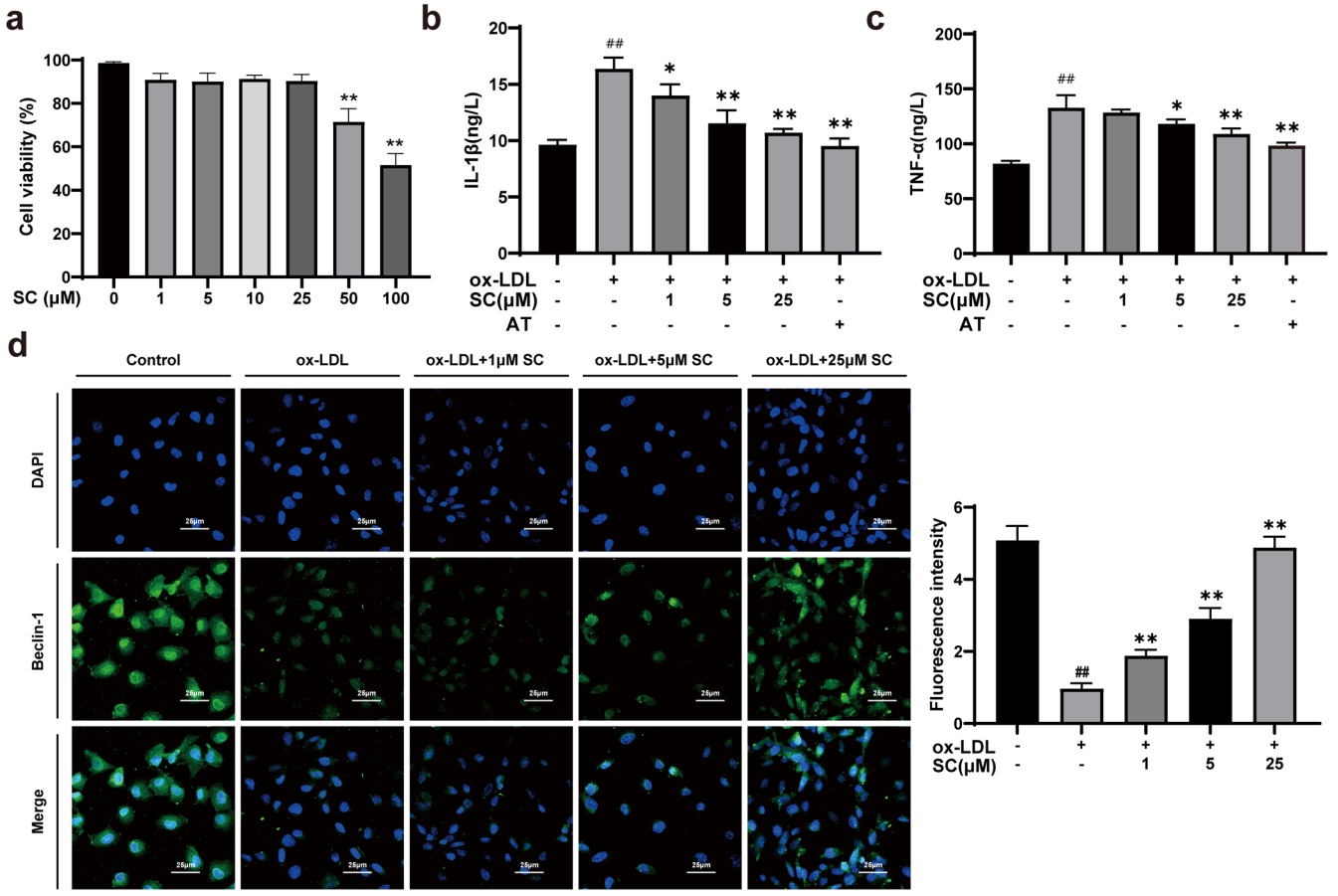

Figure 4. (a) Cell viability was detected by MTT assay; (b, c) contents of IL-Iβ and TNF-α in cell supernatant were detected by ELISA ($\bar{X} \pm S$, $n = 3$); and (d) immunofluorescence detection of Beclin1 protein, a key protein of autophagy pathway, in HUVECs (×400). Compared with the normal control group, $^{\#\#}P < 0.01$; Compared with ox-LDL group, $^{*}P < 0.05$, $^{**}P < 0.01$.

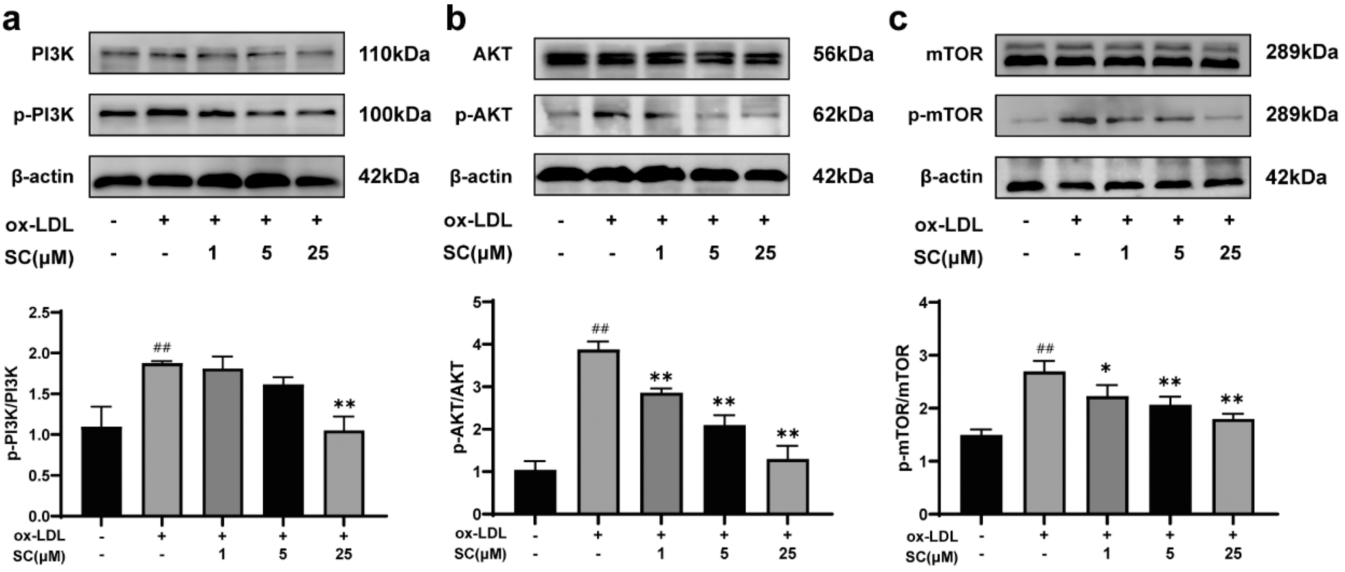

Figure 5. Effect of Schizandrin C on autophagy-related pathway protein expression in ox-LDL-induced HUVECs ($\bar{X} \pm S$, $n = 3$). (a–c) Protein expression levels of PI3K/AKT/mTOR signaling pathway. Compared with normal control group, $^{\#\#}P < 0.01$; Compared with ox-LDL group, $^{*}P < 0.05$, $^{**}P < 0.01$.

DISCUSSION

The development of atherosclerosis is closely related to a variety of risk factors, including vascular endothelial injury, inflammatory response, and abnormal lipid metabolism.[29] Recent research indicates a crucial role of autophagy in the progression of atherosclerosis in recent years. We explore the relationship between atherosclerosis and autophagy and demonstrate the

https://doi.org/10.1021/acsomega.4c03738
ACS Omega 2024, 9, 32920−32930

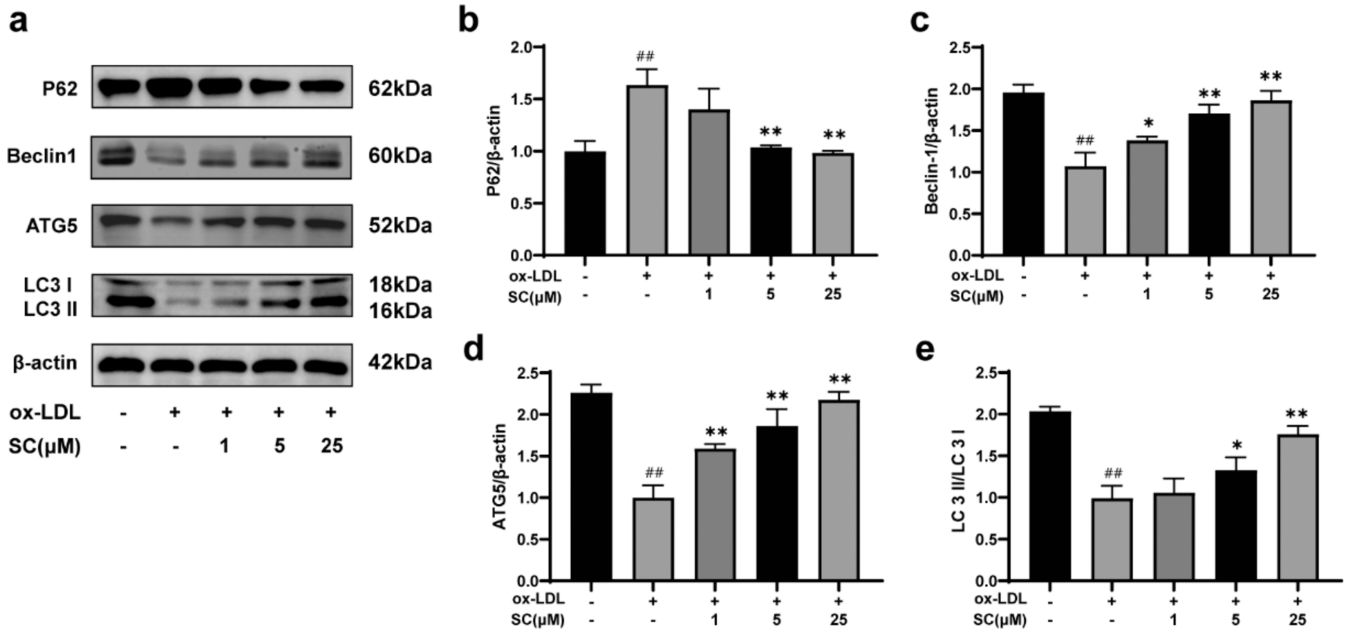

Figure 6. Expression of autophagy-related proteins in ox-LDL-induced cells induced by Schisandrin C ($\bar{X} \pm S$, $n = 3$). (a) Western blot analysis of related proteins; (b) relative protein expression of P62; (c) relative protein expression of Beclin1; (d) relative protein expression of ATG5; and (e) relative protein expression of LC3 II/LC3 I. Compared with normal control group, $^{\#\#}P < 0.01$; Compared with ox-LDL group, $^{*}P < 0.05$, $^{**}P < 0.01$.

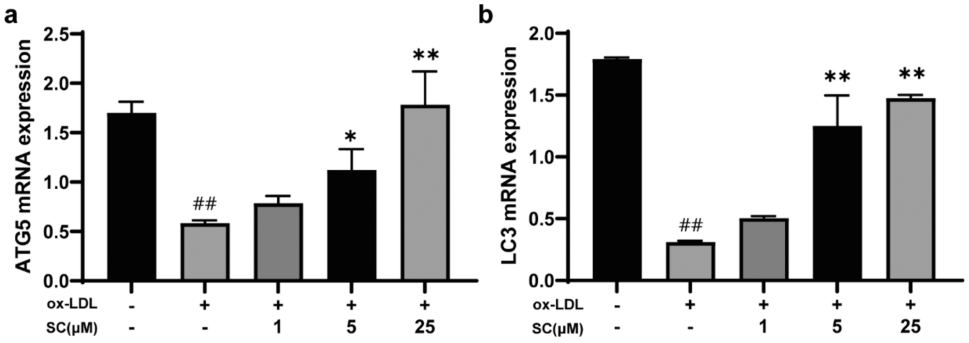

Figure 7. Effect of Schizandrin C on ATG5 and LC3 mRNA expression in ox-LDL-induced cells ($\bar{X} \pm S$, $n = 3$). (a) LC3 mRNA expression level and (b) ATG5 mRNA expression level. Compared with normal control group, $^{\#\#}P < 0.01$; Compared with ox-LDL group, $^{*}P < 0.05$, $^{**}P < 0.01$.

possible influence of autophagy on the development of atherosclerosis. Autophagy helps maintain cellular homeostasis and clear damaged proteins and organelles, and is involved in regulating cellular metabolism and stress response. First, autophagy can remove oxidative stress products and inflammatory factors within cells, thereby reducing vascular endothelial damage and inflammatory response and helping to slow down the development of atherosclerosis. Second, autophagy also regulates lipid metabolism, helping to prevent the formation of atherosclerotic plaques by clearing cholesterol and lipid deposits.[30]

Studies have shown that Schisandrin C can affect autophagy by regulating the activity of PI3K/AKT/mTOR pathway. mTOR plays an important regulatory role in autophagy and is the main negative regulatory axis of autophagy. The PI3K/Akt/ signaling pathway, which is upstream of mTOR, plays an important role in regulating mTOR and autophagy. Guided by traditional Chinese medicine, through syndrome differentiation and treatment, it regulates target organs via multiple methods, demonstrating unique advantages. It effectively treats complex diseases. A large number of traditional Chinese medicines and their active ingredients have been shown to target autophagy mediated by the PI3K/AKT/mTOR signaling pathway to inhibit inflammatory or autoimmune diseases. In order to explore the effect of SC on autophagy-related pathways, combined with network pharmacology, the role of P13K/Akt/mTOR signaling pathway in ox-LDL-induced HUVECs cells was analyzed. The results showed that ox-LDL could induce autophagy dysfunction in HUVECs, inhibit the expression of LC3 II/LC3 I, and cause endothelial injury, thus leading to the occurrence of AS. Schisandrin C can increase the expression levels of LC3 II/LC3 I in HUVECs, reduce the accumulation of ox-LDL in HUVECs and the level of p62 protein, thereby improving the autophagy flow in HUVECs and protecting endothelial cells.

In this study, the components of *Schisandra chinensis* were quantitatively analyzed, and the five active components identified by *Schisandra chinensis* were analyzed by network pharmacology. 197 key targets were predicted to be related to the treatment of atherosclerosis by *Schisandra chinensis*, and the pharmacological pathway and biological function of *Schisandra chinensis* in the treatment of atherosclerosis were determined. The core target was screened for protein interaction, and the five active components of *Schisandra chinensis* were interlinked with

https://doi.org/10.1021/acsomega.4c03738
ACS Omega 2024, 9, 32920−32930

the core target to identify the key active component as Schisandrin C. ox-LDL-induced HUVECs were used to construct atherosclerosis cell model, and different concentrations of Schisandrin C were used to intervene. The results showed that Schisandrin C could inhibit inflammatory factors and promote autophagy.

CONCLUSIONS

In summary, this study suggests that autophagy plays a crucial role in the pathogenesis of AS, and Schisandrin C can promote ox-LDL degradation by regulating the autophagy pathway mediated by PI3K/AKT/mTOR, thereby maintaining cell homeostasis. These findings suggest that increasing the level of autophagy may be a potential therapeutic strategy for the prevention and treatment of AS and provide a basis for the study of Schisandrin C in improving atherosclerosis.

ASSOCIATED CONTENT

Data Availability Statement

The data that has been used is confidential.

AUTHOR INFORMATION

Corresponding Authors

Kefeng Zhai − *School of Biological and Food Engineering, Engineering Research Center for Development and High Value Utilization of Genuine Medicinal Materials in North Anhui Province, Suzhou University, Suzhou, Anhui 234000, China; College of Biological and Food Engineering, Anhui Polytechnic University, Wuhu, Anhui 241000, China;* orcid.org/0000-0002-5198-4332; Phone: +86-557-2871681; Email: kefengzhai@163.com

Lili Li − *General Clinical Research Center, Anhui Wanbei Coal-Electricity Group General Hospital, Suzhou 234000, China;* Email: lilili07@163.com

Zhaojun Wei − *School of Biological Science and Engineering, North Minzu University, Yinchuan 750021, China;* orcid.org/0000-0003-1729-209X; Phone: +86-551-2901539; Email: zjwei@hfut.edu.cn

Authors

Hong Duan − *School of Biological and Food Engineering, Engineering Research Center for Development and High Value Utilization of Genuine Medicinal Materials in North Anhui Province, Suzhou University, Suzhou, Anhui 234000, China; College of Biological and Food Engineering, Anhui Polytechnic University, Wuhu, Anhui 241000, China*

Han Li − *School of Biological and Food Engineering, Engineering Research Center for Development and High Value Utilization of Genuine Medicinal Materials in North Anhui Province, Suzhou University, Suzhou, Anhui 234000, China; College of Biological and Food Engineering, Anhui Polytechnic University, Wuhu, Anhui 241000, China*

Tianyi Liu − *School of Biological and Food Engineering, Engineering Research Center for Development and High Value Utilization of Genuine Medicinal Materials in North Anhui Province, Suzhou University, Suzhou, Anhui 234000, China*

Yuan Chen − *School of Biological and Food Engineering, Engineering Research Center for Development and High Value Utilization of Genuine Medicinal Materials in North Anhui Province, Suzhou University, Suzhou, Anhui 234000, China; College of Biological and Food Engineering, Anhui Polytechnic University, Wuhu, Anhui 241000, China*

Mengmeng Luo − *School of Biological and Food Engineering, Engineering Research Center for Development and High Value Utilization of Genuine Medicinal Materials in North Anhui Province, Suzhou University, Suzhou, Anhui 234000, China; College of Biological and Food Engineering, Anhui Polytechnic University, Wuhu, Anhui 241000, China*

Ying Shi − *School of Biological and Food Engineering, Engineering Research Center for Development and High Value Utilization of Genuine Medicinal Materials in North Anhui Province, Suzhou University, Suzhou, Anhui 234000, China; College of Biological and Food Engineering, Anhui Polytechnic University, Wuhu, Anhui 241000, China*

Jing Zhou − *School of Biological and Food Engineering, Engineering Research Center for Development and High Value Utilization of Genuine Medicinal Materials in North Anhui Province, Suzhou University, Suzhou, Anhui 234000, China; College of Biological and Food Engineering, Anhui Polytechnic University, Wuhu, Anhui 241000, China*

Marwan M. A. Rashed − *School of Biological and Food Engineering, Engineering Research Center for Development and High Value Utilization of Genuine Medicinal Materials in North Anhui Province, Suzhou University, Suzhou, Anhui 234000, China*

Complete contact information is available at: https://pubs.acs.org/10.1021/acsomega.4c03738

Author Contributions

⊥H.D. and H.L. contributed equally. H.D.: Conceptualization, writing original draft, preparation, validation, and writing manuscript; H.L. revised this manuscript and analyzed the data; Y.S. and T.L. performed the experimental research; J.Z. and M.L. revised and edited this manuscript; M.M.A.R. and Y.C.: guided the experiment, conceptualization; L.L.: designed the experiments, revised and edited the manuscript, funding acquisition, project administration; K.Z. and Z.W.: guided the experiment, revised this manuscript, project administration. All authors have read and approved the final manuscript, and therefore, have full access to all the data in the study and take responsibility for the integrity and security of the data.

Notes

The authors declare no competing financial interest.

ACKNOWLEDGMENTS

This work was supported by the National Natural Science Foundation of China (82170481), Anhui Natural Science Foundation (2008085J39 and 2108085MH314), the Excellent top-notch Talents Training program of Anhui Universities (gxbjZD2022073), Anhui Province Innovation Team of Authentic Medicinal Materials Development and High-Value Utilization (2022AH010080), and Suzhou University Joint Cultivation Postgraduate Research Innovation Fund Project (2023KYCX06).

LIST OF ABBREVIATIONS

CVD:cardiovascular disease; AS:atherosclerosis; LDL:low-density lipoprotein; ox-LDL:oxidized low-density lipoprotein; SC:Schisandrin C; CMA:chaperone-mediated autophagy; ATG5:autophagy-related protein 5; ATG7:autophagy-related protein 7; AT:atorvastatin; IL-1β:interleukin-1β; TNF-α:tumor necrosis factor-α; AKT:protein kinase B; p-Akt:phospho-protein kinase B; PI3K:phosphoinositide 3-kinase; mTOR:-mammalian target of rapamycin; p-mTOR:phospho-mamma-

https://doi.org/10.1021/acsomega.4c03738
ACS Omega 2024, 9, 32920−32930

lian target of rapamycin; LC3:microtubule-associated protein 1 light chain 3; β-actin:β-actin; p-PI3K:phospho−phosphoinositide 3-kinase; OMIM:Online Mendelian Inheritance in Man; BP:biological process; CC:cellular component; MF:molecular function; KEGG:Kyoto Encyclopedia of Genes and Genomes; PMSF:phenylmethylsulfonyl fluorid

REFERENCES

(1) Zhao, D.; Liu, J.; Wang, M.; Zhang, X.; Zhou, M. Epidemiology of Cardiovascular Disease in China: Current Features and Implications. *Nat. Rev. Cardiol.* **2019**, *16* (4), 203−212.

(2) Riksen, N. P.; Bekkering, S.; Mulder, W. J. M.; Netea, M. G. Trained Immunity in Atherosclerotic Cardiovascular Disease. *Nat. Rev. Cardiol.* **2023**, *20* (12), 799−811.

(3) Tokgözoğlu, L.; Libby, P. The Dawn of a New Era of Targeted Lipid-Lowering Therapies. *Eur. Heart J.* **2022**, *43* (34), 3198−3208.

(4) Jonsson, A. L.; Bäckhed, F. Role of Gut Microbiota in Atherosclerosis. *Nat. Rev. Cardiol* **2017**, *14* (2), 79−87.

(5) Gisterå, A.; Hansson, G. K. The Immunology of Atherosclerosis. *Nat. Rev. Nephrol.* **2017**, *13* (6), 368−380.

(6) Nelson, K.; Fuster, V.; Ridker, P. M. Low-Dose Colchicine for Secondary Prevention of Coronary Artery Disease: JACC Review Topic of the Week. *J. Am. Coll. Cardiol.* **2023**, *82* (7), 648−660.

(7) Li, Z.; He, X.; Liu, F.; Wang, J.; Feng, J. A Review of Polysaccharides from Schisandra Chinensis and Schisandra Sphenanthera: Properties, Functions and Applications. *Carbohydr. Polym.* **2018**, *184*, 178−190.

(8) Fu, J.; Li, J.; Sun, Y.; Liu, S.; Song, F.; Liu, Z. In-Depth Investigation of the Mechanisms of Schisandra Chinensis Polysaccharide Mitigating Alzheimer's Disease Rat via Gut Microbiota and Feces Metabolomics. *Int. J. Biol. Macromol.* **2023**, *232*, No. 123488.

(9) Shen, C.; Shen, P.; Wang, X.; Wang, X.; Shao, W.; Geng, K.; Xie, H. Integrating Bioinformatics and Network Pharmacology to Explore the Therapeutic Target and Molecular Mechanisms of Schisandrin on Hypertrophic Cardiomyopathy. *Curr. Comput. Aided Drug Des.* **2023**, *19* (3), 192−201.

(10) Guo, H.-H.; Shen, H.-R.; Tang, M.-Z.; Sheng, N.; Ding, X.; Lin, Y.; Zhang, J.-L.; Jiang, J.-D.; Gao, T.-L.; Wang, L.-L.; Han, Y.-X. Microbiota-Derived Short-Chain Fatty Acids Mediate the Effects of Dengzhan Shengmai in Ameliorating Cerebral Ischemia via the Gut-Brain Axis. *J. Ethnopharmacol.* **2023**, *306*, No. 116158.

(11) Shi, X.; Han, B.; Zhang, B.; Chu, Z.; Zhang, X.; Lu, Q.; Han, J. Schisandra Chinensis Polysaccharides Prevent Cardiac Hypertrophy by Dissociating Thioredoxin-Interacting Protein/Thioredoxin-1 Complex and Inhibiting Oxidative Stress. *Biomed. Pharmacother.* **2021**, *139*, No. 111688.

(12) Feng, Y.; Li, H.; Chen, C.; Lin, H.; Xu, G.; Li, H.; Wang, C.; Chen, J.; Sun, J. Study on the Hepatoprotection of Schisandra Chinensis Caulis Polysaccharides in Nonalcoholic Fatty Liver Disease in Rats Based on Metabolomics. *Front. Pharmacol.* **2021**, *12*, No. 727636.

(13) Kim, M. R.; Cho, S.-Y.; Lee, H. J.; Kim, J. Y.; Nguyen, U. T. T.; Ha, N. M.; Choi, K. Y.; Cha, K. H.; Kim, J.-H.; Kim, W. K.; Kang, K. Schisandrin C Improves Leaky Gut Conditions in Intestinal Cell Monolayer, Organoid, and Nematode Models by Increasing Tight Junction Protein Expression. *Phytomedicine* **2022**, *103*, No. 154209.

(14) Debnath, J.; Gammoh, N.; Ryan, K. M. Autophagy and Autophagy-Related Pathways in Cancer. *Nat. Rev. Mol. Cell Biol.* **2023**, *24* (8), 560−575.

(15) Wang, L.; Klionsky, D. J.; Shen, H.-M. The Emerging Mechanisms and Functions of Microautophagy. *Nat. Rev. Mol. Cell Biol.* **2023**, *24* (3), 186−203.

(16) Yao, R.-Q.; Ren, C.; Xia, Z.-F.; Yao, Y.-M. Organelle-Specific Autophagy in Inflammatory Diseases: A Potential Therapeutic Target Underlying the Quality Control of Multiple Organelles. *Autophagy* **2021**, *17* (2), 385−401.

(17) Qiao, L.; Ma, J.; Zhang, Z.; Sui, W.; Zhai, C.; Xu, D.; Wang, Z.; Lu, H.; Zhang, M.; Zhang, C.; Chen, W.; Zhang, Y. Deficient Chaperone-Mediated Autophagy Promotes Inflammation and Atherosclerosis. *Circ. Res.* **2021**, *129* (12), 1141−1157.

(18) Zhu, T.; Li, Z.; An, X.; Long, Y.; Xue, X.; Xie, K.; Ma, B.; Zhang, D.; Guan, Y.; Niu, C.; Dong, Z.; Hou, Q.; Zhao, L.; Wu, S.; Li, J.; Jin, W.; Wan, X. Normal Structure and Function of Endothecium Chloroplasts Maintained by ZmMs33-Mediated Lipid Biosynthesis in Tapetal Cells Are Critical for Anther Development in Maize. *Mol. Plant* **2020**, *13* (11), 1624−1643.

(19) Chen, Y.; Yin, S.; Liu, R.; Yang, Y.; Wu, Q.; Lin, W.; Li, W. β-Sitosterol Activates Autophagy to Inhibit the Development of Hepatocellular Carcinoma by Regulating the Complement C5a Receptor 1/Alpha Fetoprotein Axis. *Eur. J. Pharmacol.* **2023**, *957*, No. 175983.

(20) Jia, D.; Zhang, M.; Li, M.; Gong, W.; Huang, W.; Wang, R.; Chen, Y.; Yin, Q.; Wu, J.; Jin, Z.; Wang, J.; Liu, Y.; Liang, C.; Ji, Y. NCOA4-Mediated Ferritinophagy Participates in Cadmium-Triggered Ferroptosis in Spermatogonia. *Toxicology* **2024**, *505*, No. 153831.

(21) Gao, J.-G.; Yang, J.-K.; Zhu, L.; Xu, C.; Nie, L.-W. Acrylamide Impairs the Developmental Potential of Germinal Vesicle Oocytes by Inducing Mitochondrial Dysfunction and Autophagy/Apoptosis in Mice. *Hum Exp Toxicol* **2021**, *40* (12_suppl), S370−S380.

(22) Fan, S.; Huang, Y.; Zuo, X.; Li, Z.; Zhang, L.; Tang, J.; Lu, L.; Huang, Y. Exploring the Molecular Mechanism of Action of Polygonum Capitatum Buch-Ham. Ex D. Don for the Treatment of Bacterial Prostatitis Based on Network Pharmacology and Experimental Verification. *J. Ethnopharmacol.* **2022**, *291*, No. 115007.

(23) Xu, M.; Kong, Y.; Chen, N.; Peng, W.; Zi, R.; Jiang, M.; Zhu, J.; Wang, Y.; Yue, J.; Lv, J.; Zeng, Y.; Chin, Y. E. Identification of Immune-Related Gene Signature and Prediction of CeRNA Network in Active Ulcerative Colitis. *Front. Immunol.* **2022**, *13*, No. 855645.

(24) Yuan, L.; Chu, Q.; Yang, B.; Zhang, W.; Sun, Q.; Gao, R. Purification and Identification of Anti-Inflammatory Peptides from Sturgeon (Acipenser Schrenckii) Cartilage. *Food Sci. Human Wellness* **2023**, *12* (6), 2175−2183.

(25) Li, W.; Wang, S.; Qiu, C.; Liu, Z.; Zhou, Q.; Kong, D.; Ma, X.; Jiang, J. Comprehensive Bioinformatics Analysis of Acquired Progesterone Resistance in Endometrial Cancer Cell Line. *J. Transl Med.* **2019**, *17* (1), 58.

(26) Lim, S. G.; Seo, S. E.; Park, S. J.; Kim, J.; Kim, Y.; Kim, K. H.; An, J. E.; Kwon, O. S. Real-Time Monitoring of Serotonin with Highly Selective Aptamer-Functionalized Conducting Polymer Nanohybrids. *Nano Converg.* **2022**, *9* (1), 31.

(27) Zhai, K.; Wang, W.; Zheng, M.; Khan, G. J.; Wang, Q.; Chang, J.; Dong, Z.; Zhang, X.; Duan, H.; Gong, Z.; Cao, H. Protective Effects of Isodon Suzhouensis Extract and Glaucocalyxin A on Chronic Obstructive Pulmonary Disease through SOCS3−JAKs/STATs Pathway. *Food Front.* **2023**, *4* (1), 511−523.

(28) Zhang, S.; Cai, X.; Khan, G. J.; Cheng, J.; He, J.; Zhai, K.; Mao, Y. Exploring the Molecular Mechanism of Artemisia Rupestris L. for the Treatment of Hepatocellular Carcinoma via PI3K/AKT Pathway. *J. Ethnopharmacol.* **2024**, *322*, No. 117572.

(29) Wu, J.; Zhou, Y.; Hu, H.; Yang, D.; Yang, F. Effects of β-Carotene on Glucose Metabolism Dysfunction in Humans and Type 2 Diabetic Rats. *Acta Materia Medica* **2022**, *1*, 138−153.

(30) Zhao, Y.; Xia, T.; Qiang, X.; Wang, Y.; Kang, C.; Meng, Y.; Cheng, Y.; Wang, M.; Xiao, J. Zhenjiang Aromatic Vinegar Prevents the Alcohol Liver Disease in Mice via Autophagy. *eFood* **2023**, *4* (6), No. e118.

https://doi.org/10.1021/acsomega.4c03738
ACS Omega 2024, 9, 32920−32930